Bioelectrochemistry 98 (2014) 46–52

Contents lists available at ScienceDirect

Bioelectrochemistry

journal homepage: www.elsevier.com/locate/bioelechem

Titania nanotube-modified screen printed carbon electrodes enhance the sensitivity in the electrochemical detection of proteins

Soumit S. Mandal [a,1], Vikas Navratna [b,1], Pratyush Sharma [b], B. Gopal [b], Aninda J. Bhattacharyya [a,*]

[a] Solid State and Structural Chemistry Unit, Indian Institute of Science, Bangalore 560012, India
[b] Molecular Biophysics Unit, Indian Institute of Science, Bangalore 560012, India

ARTICLE INFO

Article history:
Received 6 December 2013
Received in revised form 19 February 2014
Accepted 10 March 2014
Available online 19 March 2014

Keywords:
Electrochemical biosensor
Penicillin binding protein 2a
Methicillin resistant *Staphylococcus aureus*
Titania nanotubes

ABSTRACT

The use of titania nanotubes (TiO_2-NT) as the working electrode provides a substantial improvement in the electrochemical detection of proteins. A biosensor designed using this strategy provided a robust method to detect protein samples at very low concentrations ($C_{protein}$ ca 1 ng/μl). Reproducible measurements on protein samples at this concentration ($I_{p,a}$ of 80 ± 1.2 μA) could be achieved using a sample volume of ca 30 μl. We demonstrate the feasibility of this strategy for the accurate detection of penicillin binding protein, PBP2a, a marker for methicillin resistant *Staphylococcus aureus* (MRSA). The selectivity and efficiency of this sensor were also validated using other diverse protein preparations such as a recombinant protein tyrosine phosphatase (PTP10D) and bovine serum albumin (BSA). This electrochemical method also presents a substantial improvement in the time taken (few minutes) when compared to conventional enzyme-linked immunosorbent assay (ELISA) protocols. It is envisaged that this sensor could substantially aid in the rapid diagnosis of bacterial infections in resource strapped environments.

1. Introduction

The rapid and accurate identification of drug resistant bacteria is crucial to control the outbreak of bacterial infection in hospitals. This is particularly relevant in the case of *Staphylococcus aureus*, a leading cause of high morbidity and mortality in both community and hospital associated infections [1]. An acquired penicillin binding protein, PBP2a, is a prominent biomarker to distinguish Methicillin-resistant *Staphylococcus aureus* (MRSA) from Methicillin-sensitive *S. aureus* (MSSA) [2]. The detection of PBP2a at the gene, mRNA and protein levels has been extensively examined to distinguish MRSA from MSSA. These detection strategies vary substantially in terms of the duration, sensitivity, sophistication and the infrastructure requirements. One of the methods for the detection of PBP2a at the DNA level involves an integrated microfludic system that performs a multistep assay in a single disposable fluidic cartridge, resulting in simultaneous detection of the genes encoding the virulence factor Panton Valentine leukocidin (PVL), femA protein, protein A and PBP2a [3]. Detection of mRNAs from bacterial cultures is another approach that aids in evaluating the expression levels of representative biomarkers [4]. The most cost-effective method however is protein based. This involves the detection of PBP2a from MRSA cell extracts. Almost all currently available protocols for PBP2a identification rely on enzyme linked immunosorbent assays (ELISA) [5] or variants like the bioluminescent enzyme immunoassay (BLEIA) [6], rapid latex agglutination assay [7], radioimmunoassay [8], chemiluminescence assay [9] or the immune-polymerase chain reaction assay [10]. Protein based methods have an inherent drawback due to the stability of the protein sample and the dynamic range of detection [11–13]. Indeed protein levels vary widely between cells and are sensitive to changes in the sample preparation protocol. (See Scheme 1.)

Electrochemical methods for the detection of proteins are faster than conventional biochemical strategies. The small detection volumes, reusability and ease of storage render these methods simple and cost effective. Furthermore, electrochemical methods are amenable for high throughput measurements as the efficiency of electrochemical detection can be substantially enhanced by the use of appropriate nanostructured materials [14]. The integration of nanostructured metals or metal oxides on the carbon layer of the working electrode introduces diversity in the physical (electronic, photonic and catalytic) properties. These variations can be exploited to optimize the performance of the working electrode [15–19]. The nanostructured metal/metal oxide particles also have a very high surface to volume ratio. The larger effective surface area allows more biomolecules to be immobilized at or near the electrode surface. This reduces the distance for electron transfer between the biomolecule and the metal/metal oxide particles. As a result, the charge transfer to the electrodes becomes easier. In addition, the strong interactions between the biomolecule and modified electrode surface increase the surface density of the adsorbed protein [20].

* Corresponding author. Fax: +91 80 23601310.
[1] Soumit S. Mandal and Vikas Navratna have contributed equally to the work.

http://dx.doi.org/10.1016/j.bioelechem.2014.03.003
1567-5394/

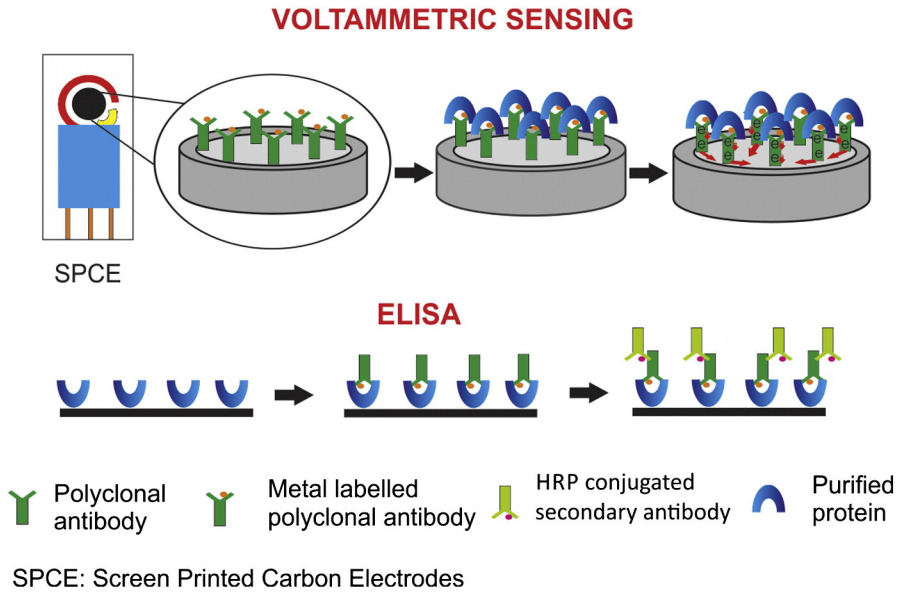

Scheme 1. Schematic representation of the electrochemical sensor. (A). Nanostructured oxide modified screen printed carbon electrodes coated with metal labeled antibodies. Two proteins (*S. aureus* PBP2a and *D. melanogaster* PTP10D) were examined. (B) Detection of identically prepared protein samples using ELISA. For ease in comparison, metal tagged antibodies were employed in this assay.

In this study, we demonstrate the feasibility of a titania-nanotube (TiO_2-NT) modified carbon electrode as the working electrode in an electrochemical biosensor to enhance the sensitivity in protein detection. Titania was chosen for the modification of the working electrode surface due to its biocompatibility and exceptional electrical properties [21]. The performance of this titania nanotube biosensor was found to be comparable or better than ELISA-based methods with the added advantage of much lower sample volumes and rapid detection.

2. Experimental: materials and methods

2.1. Protein purification

The recombinants *S. aureus* PBP2a and *Drosophila melanogaster* PTP10D were obtained by overexpression in *Escherichia coli*. The plasmids encoding PBP2a and PTP10D were transformed into BL21(DE3) cells. The recombinant proteins from these expression cells were purified by immobilized metal affinity chromatography (IMAC) using Ni^{2+}-nitrilotriacetic acid (Ni^{2+}-NTA) affinity beads (Sigma-Aldrich Co.) and ion exchange chromatography. The subsequent steps of purification and variations in the buffer composition in these steps are described in relevant references [22,23]. The purity of recombinant protein was examined by sodium dodecyl sulfate poly acrylamide gel electrophoresis (SDS-PAGE) (Supplementary Fig. 1).

2.2. Preparation of E. coli cell free lysate

The plasmid containing the gene encoding *S. aureus* PBP2a was transformed into *E. coli* BL21(DE3) pLysS cells. A single transformed colony was inoculated into 7 ml of LB media containing kanamycin. Cells were grown at 37 °C to an optical density of 0.6 at 600 nm. The cells were subsequently distributed into seven aliquots of 1 ml each. The *E. coli* cultures were induced with varying concentrations of Isopropyl β-D-1-thiogalactopyranoside (IPTG) (C_{IPTG}; 0–0.4 mM final concentration). Post induction, the cells were further grown at 37 °C for 2–3 h. Simultaneously, 1 ml of untransformed culture was also grown under similar experimental conditions. The cells were pelleted and resuspended in 100 μl of buffer (100 mM Tris-HCl, pH 7.5). The resuspended culture was lysed, centrifuged and the supernatant was collected and used in the electrochemical experiments.

2.3. Preparation of DTPA anhydride

Diethylene triamine pentaacetic acid (DTPA) anhydride was prepared as described earlier [24]. DTPA (1.96 g, 0.01 mol) and triethylamine (3.5 ml, 0.05 mol) were dissolved in dry acetonitrile by stirring at 60 °C for 1 h. The reaction mixture was cooled to room temperature and 5 ml of this mixture was further cooled to 0 °C in a vial with a rubber stopper. Isobutyl chloroformate (0.5 mmol) was added to the cooled reaction mixture. The solution was allowed to stand in an ice bath for 1.5 h after shaking it well. Later, the sample was flash frozen and stored at −80 °C.

2.4. Polyclonal antibody generation, purification and labeling

The purified recombinant proteins were used to raise polyclonal antibodies in New Zealand white rabbits. Briefly, blood samples were collected and allowed to clot at 4 °C for 24–30 h and the serum was retrieved by centrifugation at 3000 rpm for 30 min. The serum was stored at −20 °C. Antibodies from serum were purified by ammonium sulfate precipitation and were subsequently tagged with the metal ion. The procedure adapted for metal ion conjugation to antibody was adapted from a protocol described earlier [24]. Briefly, Diethylene triamine pentaacetic acid (DTPA) anhydride was reacted with 300 μg of antibody in 0.1 M phosphate buffer at pH 7.5 for 2 h at room temperature. The reaction mixture was later cooled in an ice bath and 50 μl of 50 mM $FeCl_3$ was added to the 1 ml cooled mixture and allowed to stand in an ice bath for 10 min. The reaction mixture was then neutralized with 300 μl of 0.1 M phosphate buffer (pH 7.5) for 5 min and the antibody thus labeled was further purified by passing it through a 10 ml Sephadex G-50 size exclusion chromatography column (Sigma-Aldrich Co.) (Supplementary Fig. 2). The purified metal tagged antibodies were subjected to inductively coupled plasma atomic emission spectroscopy (ICPAES) analysis and the presence of Fe (III) was confirmed (Supplementary Fig. 4). These modified antibodies are referred to as Fe (III)-tagged anti-PBP2a and Fe (III)-tagged anti-PTP10D in the subsequent discussion.

2.5. Enzyme linked immunosorbent assay (ELISA)

The ELISA plates (F16 Maxisorp Nunc Immuno Module) were coated with varying amounts of purified recombinant protein (either PBP2a or PTP10D) by incubating the wells with protein in 100 μl of 1X phosphate buffered saline (PBS) pH 7.5, overnight at 4 °C. The plates were washed with phosphate buffered saline with Tween-20 (PBST) and blocking was performed by incubating the wells with 100 μl of 3% skim milk powder (Hi-Media Inc.) and 0.05% Tween-20 (SIGMA Aldrich) in 1X PBS at room temperature for 1 h. The plates were then washed with PBST and 100 μl purified primary antibody was added (1:100 dilution). At this step, the plates were incubated overnight at 4 °C. The following day, plates were washed with PBST and 100 μl (1:10,000 dilutions) of horse radish peroxidase conjugated anti-rabbit IgG raised in goat (Bangalore Genei, Inc.). This was subsequently incubated at room temperature for 1 h. Later, the plates were washed with 1X PBST and the reaction was developed by adding 100 μl of 0.2 mg/ml 2, 2′-azinobis(3-ethylbenzothiazoline-6-sulphonic acid) (ABTS) with 0.003% hydrogen peroxide in 50 mM sodium citrate buffer, pH 4.0 and incubating the reaction mixture in dark for 30 min. The absorbance was measured at 405 nm.

2.6. Preparation of titania nanotubes (TiO_2-NT)

The titania nanotubes (TiO_2-NT) used for preparing the modified electrodes were synthesized using a standard hydrothermal method [25]. 1 g of commercially available Degussa P25 TiO_2 nanoparticles was stirred in 40 ml of 10 M aqueous sodium hydroxide (NaOH) solution for approximately 2 h. This was followed by heating this solution at 130 °C for 72 h in Teflon lined stainless steel autoclave. The reaction mixture was then cooled to 25 °C and the product was recovered via centrifugation followed by washing with 0.1 M HCl solution and deionized water several times until the sample stabilized at pH 7. The product was dried at 100 °C and then annealed at 400 °C for 5 h.

2.7. Sensor fabrication and measurements

The electrochemical measurements were carried out with a potentiostat (Dropsens, μstat 400) using screen printed carbon electrodes (SPCEs). The SPCE substrate was ceramic (dimensions: length 33 mm; width 10 mm; height 0.5 mm). In the SPCE, the working (4 mm diameter) and counter electrodes were made of carbon while the reference was made up of silver. Before use, the SPCEs were pretreated by cyclic voltammetry (CV) between 0 and 1.4 V in 1 M H_2SO_4 until a stable signal was obtained and this was followed by CV in 0.1 M $K_3[Fe(CN)_6]$ solution. The SPCEs were thoroughly washed with millipore water and incubated in water overnight to ensure complete cleaning. The modified working electrode was prepared by the drop casting method which is extensively used for the preparation of modified electrode [26–30]. 20 μl of titania nanotubes (TiO_2-NT, 10 mg/ml) was drop cast on SPCE. This was followed by the attachment of anti-PBP2a or anti-PTP10D antibodies to the pre-treated nanotubes. The electrodes were dried overnight after each step to ensure proper attachment of the TiO_2-NT with the antibodies. In these electrochemical measurements, the volume of the PBP2a and PTP10D proteins were varied during the cyclic voltammetry recording while keeping the total volume restricted to 30 μl.

3. Results and discussion

Cyclic voltammetry (CV) is an effective method to detect electroactive molecules [31]. It provides a direct route to measure analyte concentration in solution in terms of peak current (I_p) at a standard redox potential. In this study, titania-modified carbon screen printed working electrodes were employed for electrochemical detection. These titania nanotubes (TiO_2-NT) (Fig. 1A) were obtained from an optimized hydrothermal synthesis [25]. The typical dimensions of these titania nanotube were-length: ca 100–150 nm, inner diameter: ca 5–6 nm and outer diameter: ca 10 nm. The XRD pattern (supplementary Fig. 3) of these nanotubes reveals the presence of a mixed phase comprising of anatase and TiO_2-B [32]. The surface nature of the bare and modified SPCE was determined from the contact angle measurements shown in Fig. 1B and C. The contact angle for bare SPCE was found to be 120° while that for the TiO_2 nanotube (TiO_2-NT) modified SPCE was 10°. These values suggest that the highly hydrophobic nature of bare SPCE transforms to hydrophilic upon modification with TiO_2-NT. The bare and TiO_2-NT modified SPCE were employed for the detection of the $Fe^{3+} \leftrightarrow Fe^{2+}$ redox couple within a voltage range −0.6–1.0 V at a scan rate (ν) of 100 mV s^{-1}. A higher scan rate was selected in order to achieve a higher current response ($I_p \propto \nu^{0.5}$) and rapid detection.

The purified metal tagged antibodies contained 13–15 μM of metal ions per μM of antibody (13.2 μM per μM of anti-PBP2a and 15 μM per μM of anti-PTP10D; Supplementary Fig. 4). Optimal amounts of titania nanotube and Fe (III)-tagged anti-PBP2a in Tris(hydroxymethyl) aminomethane (Tris)-HCl buffer (pH 7.5) were dropcasted on SPCE and dried. The dried layer (comprising titania nanotube and Fe (III)-tagged anti-PBP2a) formed the working electrode and the biorecognition layer of the electrochemical sensor. Fig. 2A (inset) shows a comparison of the cyclic voltammogram of Fe (III)-tagged anti-PBP2a with aqueous (200 μM) $FeCl_3$ solution using TiO_2-NT. The $FeCl_3$ solution showed the expected reversible response pertaining to the $Fe^{3+} \leftrightarrow Fe^{2+}$ redox couple. On the other hand, the reaction involving the Fe (III)-tagged anti-PBP2a was not reversible and the peak current ($I_{p,a}$) was of lower magnitude and shifted more towards the negative potential when compared to $FeCl_3$. This finding could also be reproduced in the case of the Fe (III)-tagged anti-PTP10D antibody. The decrease in current and the absence of a reversible response were attributed to the coordination environment of the Fe (III) ion in the protein. The Fe (III) ion is likely to be buried in a hydrophobic environment which could act as a barrier for the diffusion of electrons [33]. These electrochemical characteristics are similar to heme proteins like hemoglobin [34–36].

The interaction of the antibody (Fe (III)-tagged anti-PBP2a) with the antigen (purified recombinant PBP2a; experimental methods and supplementary Fig. 1) results in detectable change in the current response

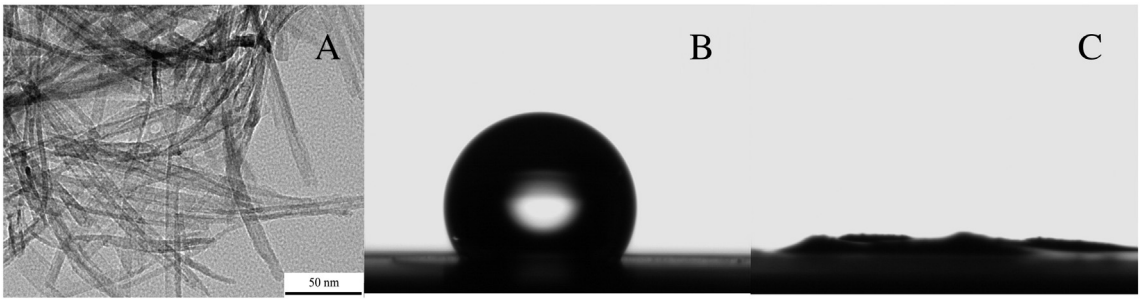

Fig. 1. (A) Transmission electron micrographs of titania nanotubes (TiO_2-NT). Contact angle measurement on (B) bare SPCE (C) titania nanotubes (TiO_2-NT) modified SPCE.

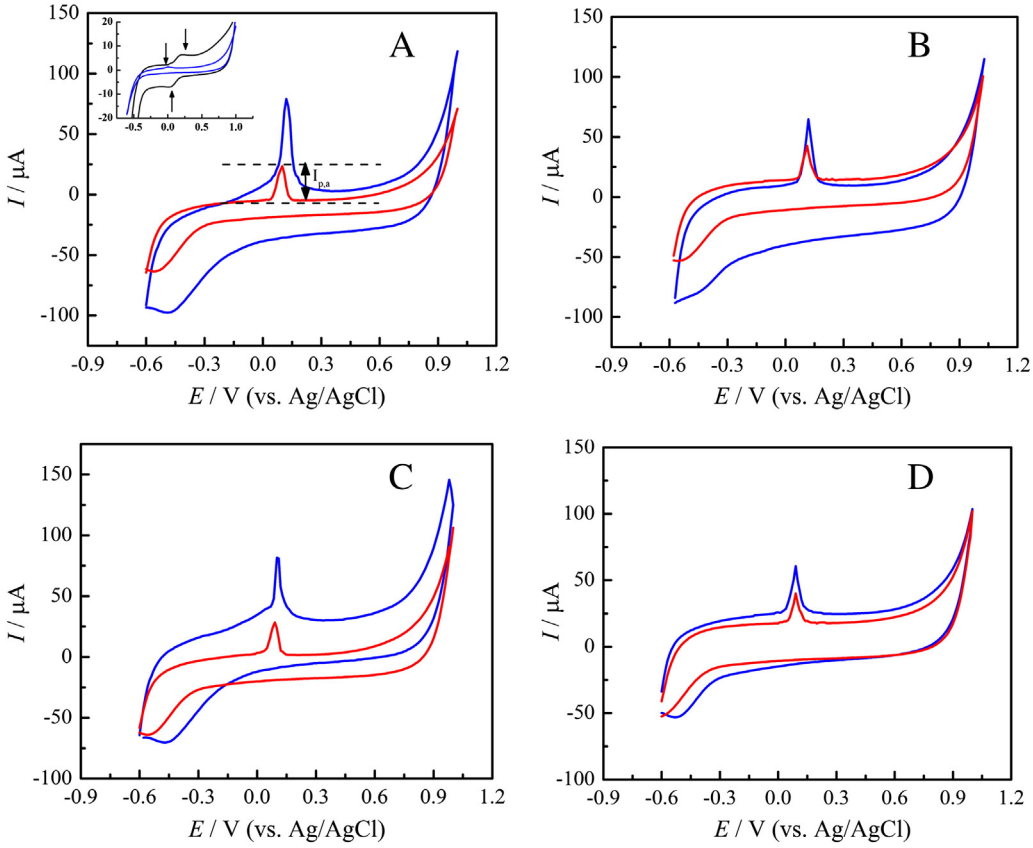

Fig. 2. (A) Cyclic voltammogram of Fe (III)-tagged anti-PBP2a (blue) and Fe (III)-tagged anti-PBP2a-PBP2a (red) on TiO_2-NT modified SPCE and (B) bare SPCE. Inset: cyclic voltammogram of 200 µM $FeCl_3$ salt (black) and Fe-tagged anti-PBP2a (blue). (C) Cyclic voltammogram of Fe (III)-tagged anti-PTP10D (blue) and Fe (III)-tagged anti-PTP10D-PTP10D (red) on TiO_2-NT modified SPCE and (D). bare SPCE. A scan rate of 100 mVs^{-1} was maintained for all the measurements.

(Fig. 2A). The changes in current are due to the variation in the redox potential caused by specific antibody–antigen interaction. The change in current response was monitored as a function of the concentration of PBP2a antigen (C_{PBP2a}). This allowed us to estimate the sensitivity and detection limit of the TiO_2-NT working electrode of the sensor. Fig. 2A shows the voltammogram obtained upon the addition of the antigen (ca 60 ng/µL) to the Fe (III)-tagged anti-PBP2a activated TiO_2-NT electrodes. Fig. 2B shows the variation in current response as a result of the addition of PBP2a to Fe (III)-tagged anti-PBP2a immobilized on to bare SPCE. We note that the anodic peak current decreases substantially in the case of specific antibody–antigen interaction. The decrease is higher for the TiO_2-NT modified electrodes.

This finding is consistent with experiments involving Fe (III)-tagged anti-PTP10D and the cognate antigen (purified recombinant PTP10D) on TiO_2-NT modified (Fig. 2C) and unmodified SPCE (Fig. 2D). The peak current ($I_{p,a}$) decreased as a function of increasing PTP10D (antigen) concentration (C_{PTP10D}; 1–100 ng/µl). The decrease in current (Fig. 3A and C) with increasing protein concentration could be attributed to the progressive binding of the cognate proteins to the antibody. It is likely that the addition of antigen leads to the gradual occlusion of the Fe-center of antibodies into a hydrophobic environment resulting in a decrease in the current response ($I_{p,a}$). In addition, the charge transfer resistance also increases linearly with an increase in the protein concentration [37]. A likely explanation for this observation could be that a substantial proportion of the protein sample is localized at the electrode surface. This acts as an insulating barrier for electron transport. Thus a decrease in current response ($I_{p,a}$) as a function of protein concentration is a combination of both, an inaccessible Fe-center and insulation of the electrode surface. Despite these apparent limitations, the current response at low protein concentration (100 ng/µl) is few tens of microamperes higher than the lower limit (in the range of ca 10^{-12} A) of modern potentiometers (Fig. 3A and B).

The modification of SPCE by TiO_2-NT effectively alters the electronic properties of the working electrode and also increases the effective surface area for the electrochemical reaction. This TiO_2-NT modified SPCE could detect very low concentrations (1–4 ng/µl) of PBP2a (C_{PBP2a}) (Fig. 3B). This increase in the sensitivity of the working electrode is due to the ability of TiO_2-NTs to reduce the background current response arising from the buffer (typical ionic strength of 0.1 M) while providing an electrical conduit for the facile flow of the electrons from the protein to the carbon electrode surface [38]. Indeed, attempts to detect low concentrations PBP2a (C_{PBP2a}: 1–4 ng/µl) with bare carbon electrodes were unsuccessful primarily due to the inability of the carbon electrode to negate the buffer effect [39]. Furthermore, the presence of the TiO_2-NT on carbon prevents the adsorption of the protein directly on the working electrode surface and avoids formation of the insulating layer. These observations were also supported by results from the experiments involving Fe (III)-tagged anti-PTP10D. Fig. 3C shows a decrease in current response as a function of increasing PTP10D concentrations (C_{PTP10D}). Protein concentrations as low as 0.5 ng/µl (Fig. 3D) could be detected. Thus, the TiO_2-NT modification of SPCE helps in enhancing the detection range and efficiency of the sensor.

To ascertain specificity in detection, control experiments were performed by swapping the interacting antigenic proteins. It was observed that the decrease in the anodic peak current ($I_{p,a}$) arising from the nonspecific binding of PTP10D to Fe (III)-tagged anti-PBP2a was lower when compared to the selective binding of PBP2a to Fe (III)-tagged anti-PBP2a (Fig. 2A). Similarly, the decrease in the anodic peak current ($I_{p,a}$) arising due to the nonspecific binding of PBP2a to Fe (III)-tagged anti-PTP10D was less when compared to the selective binding of

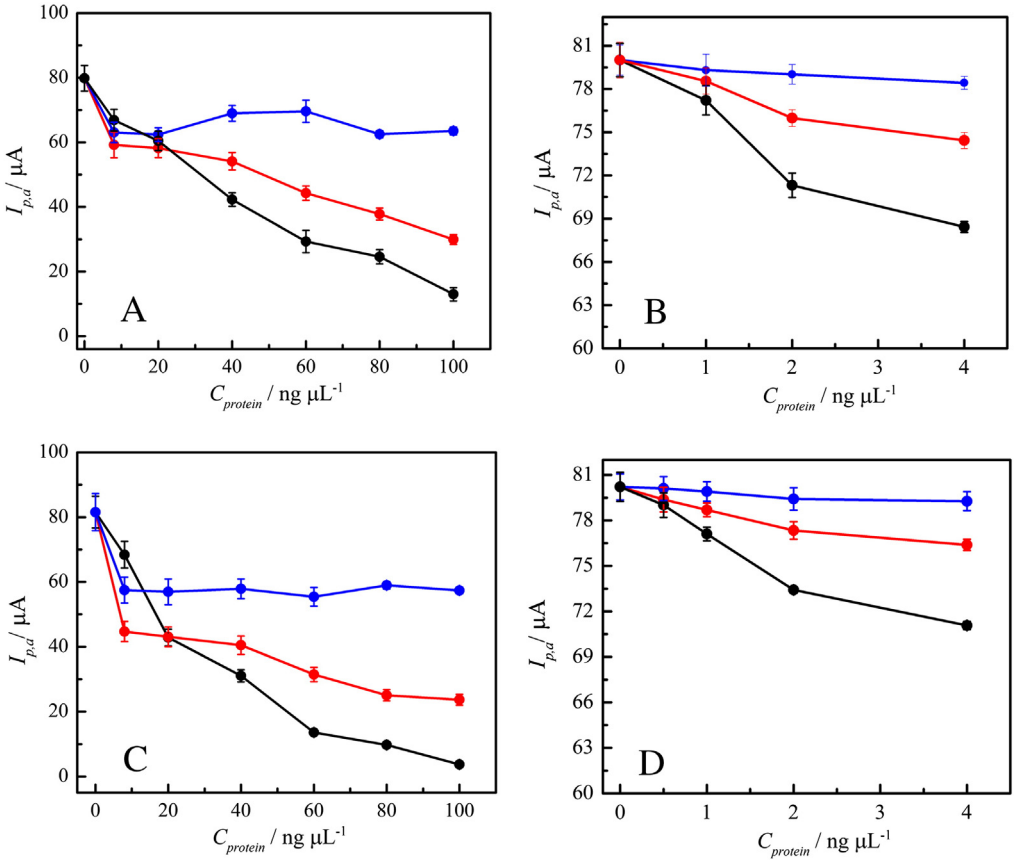

Fig. 3. Variation of anodic peak current response ($I_{p,a}$) as a function of protein concentrations arising from antigen–antibody interactions (A) Interaction of Fe (III)-tagged anti-PBP2a with PBP2a (black); PTP10D (red); BSA (blue) using bare SPCE (B): Variation of anodic peak current as a function of PBP2a (black), PTP10D (red); BSA (blue) concentration in the range 1–4 ng µL^{-1} using (TiO_2-NT) modified SPCE (C) Interaction of Fe(III)-tagged anti-PTP10D with PTP10D (black); PBP2a (red); BSA (blue) using bare SPCE (D): Variation of anodic peak current as a function of PTP10D PBP2a (red); BSA (blue) concentration in the range 0.5–4 ng µL^{-1} using TiO_2-NT modified SPCE.

PTP10D to Fe (III)-tagged anti-PTP10D (Fig. 2B). These experiments were performed on unmodified SPCE with protein concentrations (C_{PTP10D} or C_{PBP2a}) that varied from 8 to 100 ng/µl. The specificity was further cross checked in the lower concentration range using the TiO_2-NT modified SPCE (Fig. 3B and D). It appears likely that the cross-reactivity (albeit minimal) is likely due to the fact that both antibodies used in this study were polyclonal antibodies. Additional specificity can thus be engineered by the use of monoclonal antibodies with appropriate epitope specificity for specialized applications.

In addition, bovine serum albumin (BSA) was also used as a control protein to check the specificity of the antibodies towards its cognate antigen under identical experimental conditions. Fe (III)-tagged anti-PBP2a and Fe (III)-tagged anti-PTP10D on bare SPCE were exposed to varying concentrations (8–100 ng/µl) of BSA (C_{BSA}) in Tris-HCl buffer. Similarly, Fe(III)-tagged antibodies on TiO_2-NT modified SPCE were also exposed to low concentrations of BSA (C_{BSA}: 1–4 ng/µl). The peak current response ($I_{p,a}$) upon binding of BSA remained fairly constant irrespective of BSA concentration (Fig. 3A–D) in these experiments. The nearly independent current response vis-a-vis BSA concentration (C_{BSA}) could be attributed to the nonspecific binding of BSA to the Fe (III)-tagged anti-PBP2a/PTP10D.

In another experiment, cell free lysates of *E. coli* expressing different amounts of PBP2a were used in lieu of the purified antigen. Increasing the level of the inducer (IPTG) in cells over-expressing PBP2a resulted in lysates that had different levels of recombinant PBP2a. This change in the level of PBP2a was reflected in the electrochemical experiments (Supplementary Fig. 5). The linearity of the response emphasizes the selective binding of Fe (III)-tagged anti-PBP2a with PBP2a in the cell free lysate. Similar experiments were performed with PTP10D.

ELISA experiments were also performed using purified recombinant proteins. The antigen (*S. aureus* PBP2a/*D. melanogaster* PTP10D) was immobilized on the ELISA plate at different concentrations. The plates were incubated with the cognate antibodies (anti-PBP2a and anti-PTP10D). Horse radish peroxidase (HRP) conjugated anti-rabbit IgG was used as secondary antibody. The HRP conjugation to the secondary antibody utilized 2, 2′-azino-bis(3-ethylbenzothiazoline-6-sulphonic acid) (ABTS) as substrate and could be measured at 405 nm. The absorbance values thus obtained were used to estimate varying antigen concentrations. Concentrations of proteins as low as 0.3–10 ng/µl could be detected using both metal labeled anti-PBP2a and anti-PTP10D (Fig. 4A and B). The values obtained from the indirect ELISA experiments could be reproduced with minimal experimental errors. It was observed that variation in the incubation time and temperature affected the sensitivity in detection (data not shown). For the ease of obtaining concentration estimations directly from the plot, the log of protein concentrations was plotted versus absorbance value to obtain a linear plot. The sensitivity in these measurements compares favorably with the electrochemical detection method. However, ELISA is time consuming, indirect and employs extensive protocols for the estimation of protein concentration. Enhancement in the sensitivity of ELISA can be achieved by varying the chromophore or fluorophore labels on the secondary antibody — a process that is both expensive and time-consuming [39,40]. On the other hand, the sensitivity of the electrochemical strategy can be further enhanced by using monoclonal antibodies as opposed to the polyclonal antibodies raised against the recombinant proteins.

The specificity of the electrochemical protein detection method was also compared with conventional ELISA. To estimate the level of interference from non-specific interactions, these experiments were performed using cell free lysates. It was observed that the electrochemical

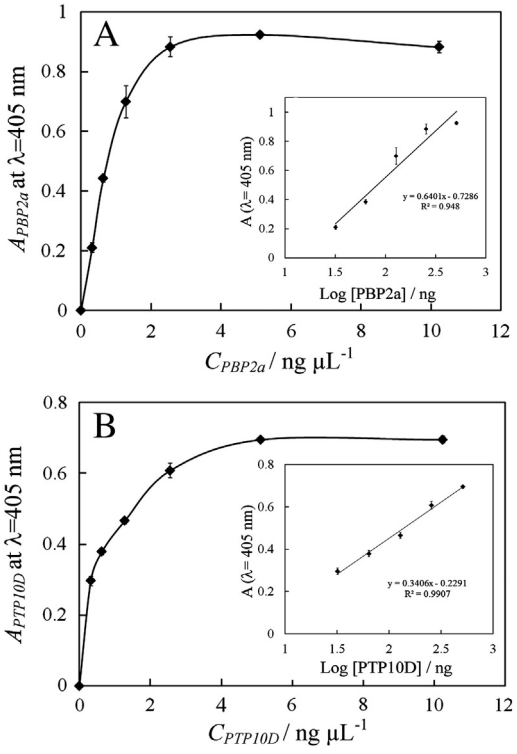

Fig. 4. Antigen detection using conventional ELISA (A) Varying concentrations of PBP2a detected using polyclonal anti-PBP2a antibodies. (B) Varying concentrations of PTP10D detected using polyclonal anti-PTP10D antibodies. A minimum of 0.3 ng μL^{-1} of the protein could be detected. HRP conjugated anti-rabbit IgG was used as the secondary antibody. Standard plots for the estimation of recombinant PBP2a (Inset A) and recombinant PTP10D (Inset B) concentration using ELISA were generated by plotting the log of protein concentration (on x-axis) versus the absorbance at 405 nm. A is the absorbance.

method is more efficient than ELISA in the specific detection of an antigen in a crude cell lysate. An inherent limitation is the low absorbance values recorded in ELISA experiments. The differences in these readings between different samples are thus prone to significant errors. The electrochemical method of detection, however, revealed a significant current response. This comparison is shown in supplementary Fig. 5.

4. Conclusion

A titania nanotube modified-SPCE based electrochemical sensor could reproducibly detect target proteins at concentrations as low as 1–10 ng μl^{-1}. The sensitivity and linearity in the electrochemical sensing method suggest that the current measurements can be directly correlated to the concentration of the antigenic protein. The feasibility of this strategy suggests that the detection range can be further enhanced by optimization of the surface area or electronic properties of the nanostructured electroactive layer. Further analysis using oxides instead of noble metals such as gold in the bio-recognition layer appears to be a potential route to enhance the cost-effectiveness of an electrochemical biosensor. The use of controlled nanostructures in an electrochemical method thus reveals a route to robust biosensors for the rapid detection of target antigenic proteins in diverse clinical applications.

Appendix A. Supplementary data

Supplementary data to this article can be found online at http://dx.doi.org/10.1016/j.bioelechem.2014.03.003.

References

[1] K. Schleifer, Taxonomy of coagulase-negative staphylococci, in: P.A. Mardt, K.H. Schleifer (Eds.), Coagulase-Negative Staphylococci, Almqvist and Wiksell International, Stockholm, Sweden, 1986, pp. 11–26.
[2] T.R. Walsh, R.A. Howe, The prevalence and mechanisms of vancomycin resistance in *Staphylococcus aureus*, Annu. Rev. Microbiol. 56 (2002) 657–675.
[3] Y.W. Chen, H. Wang, M. Hupert, S.A. Soper, Identification of methicillin-resistant *Staphylococcus aureus* using an integrated and modular microfluidic system, Analyst 138 (2013) 1075–1083.
[4] R.M. Anthony, A.R.J. Schuitema, L. Oskam, P.R. Klatser, Direct detection of *Staphylococcus aureus* mRNA using a flowthrough microarray, J. Microbiol. Methods 60 (2005) 47–54.
[5] E. Engvall, P. Perlmann, Enzyme linked immunosorbent assay (ELISA). Quantitative assay of immunoglobulin G, Immunochemistry 8 (1971) 871–874.
[6] K. Shiga, K. Gomi, M. Nishimura, M. Watanabe, F. Nomura, N. Kajiyama, Discrimination of methicillin-resistant *Staphylococcus aureus* from methicillin-susceptible *Staphylococcus aureus* or coagulase-negative staphylococci by detection of penicillin-binding protein 2 and penicillin-binding protein 2′ using a bioluminescent enzyme immunoassay, J. Immunol. Methods 388 (2013) 40–45.
[7] Y. Nakatomi, J. Sugiyama, Rapid latex agglutination assay for the detection of penicillin-binding protein 2′, Microbiol. Immunol. 42 (1998) 739–743.
[8] S.J. Goldsmith, Radioimmunoassay: review of basic principles, Semin. Nucl. Med. 5 (1975) 125–152.
[9] Z. Fu, C. Hao, X. Fei, H. Ju, Flow-injection chemiluminescent immunoassay for alpha-fetoprotein based on epoxysilane modified glass microbeads, J. Immunol. Methods 312 (2006) 61–67.
[10] K. Saito, D. Kobayashi, M. Sasaki, H. Araake, T. Kida, A. Yagihashi, T. Yajima, H. Kameshima, N. Watanabe, Detection of human serum tumor necrosis factor-alpha in healthy donors, using a highly sensitive immuno-PCR assay, Clin. Chem. 45 (1999) 665–669.
[11] B.G. Hoffstrom, E.A. Wayner, Immunohistochemical techniques to study the extracellular matrix and its receptors, Methods Enzymol. 245 (1994) 316–346.
[12] K. Chandramouli, P.-Y. Qian, Proteomics: challenges, techniques and possibilities to overcome biological sample complexity, Hum. Genomics Proteomics (2009) 1–22.
[13] M. Bunea, O. Zarnescu, New current aspects on the immunohistochemical techniques, Roum. Biotechnol. Lett. 6 (2001) 177–206.
[14] M.C. Daniel, D. Astruc, Gold nanoparticles: assembly, supramolecular chemistry, quantum-size-related properties, and applications toward biology, catalysis, and nanotechnology, Chem. Rev. 104 (2004) 293–346.
[15] J.P. Metters, F. Tan, R.O. Kadara, C.E. Banks, Electroanalytical properties of screen printed shallow recessed electrodes, Anal. Methods 4 (2012) 3140–3149.
[16] J.P. Metters, R.O. Kadara, C.E. Banks, New directions in screen printed electroanalytical sensors: an overview of recent developments, Analyst 136 (2011) 1067–1076.
[17] J.-M. Zen, A.S. Kumar, D.-M. Tsai, Recent updates of chemically modified electrodes in analytical chemistry, Electroanalysis 15 (2003) 1073–1087.
[18] J. Wang, N. Naser, L. Angnes, H. Wu, L. Chen, Metal-dispersed carbon paste electrodes, Anal. Chem. 64 (1992) 1285–1287.
[19] I. Willner, E. Katz, Integrated nanoparticle–biomolecule hybrid systems: synthesis, properties, and applications, Angew. Chem. Int. Ed. 43 (2004) 6042–6108.
[20] J. Zhao, R.W. Henkens, J. Stonehuerner, J.P. O'Daly, A.L. Crumbliss, Direct electron transfer at horseradish peroxidase-colloidal gold modified electrodes, J. Electroanal. Chem. 327 (1992) 109–119.
[21] X. Chen, S.S. Mao, Titanium dioxide nanomaterials: synthesis, properties, modifications, and applications, Chem. Rev. 107 (2007) 2891–2959.
[22] L.L. Madan, B. Gopal, Conformational basis for substrate recruitment in protein tyrosine phosphatase 10D, Biochemistry 50 (2011) 10114–10125.
[23] C. Fuda, M. Suvorov, S.B. Vakulenko, S. Mobashery, The basis for resistance to beta-lactam antibiotics by penicillin-binding protein 2a of methicillin-resistant *Staphylococcus aureus*, J. Biol. Chem. 279 (2004) 40802–40806.
[24] C.H. Palk, P.R. Murphy, W.C. Eckelman, W.A. Volkert, R.C. Reba, Optimization of the DTPA mixed-anhydride reaction with antibodies at low concentration, J. Nucl. Med. 24 (1983) 932–936.
[25] S.K. Das, A.J. Bhattacharyya, High lithium storage in mixed crystallographic phase nanotubes of titania and carbon–titania, J. Phys. Chem. C 113 (2009) 17367–17371.
[26] M. Yemini, M. Reches, J. Rishpon, E. Gazit, Novel electrochemical biosensing platform using self-assembled peptide nanotubes, Nano Lett. 5 (2005) 183–186.
[27] X. Lu, Y. Xiao, Z. Lei, J. Chen, H. Zhang, Y. Ni, Q. Zhang, A promising electrochemical biosensing platform based on graphitized ordered mesoporous carbon, J. Mater. Chem. 19 (2009) 4707–4714.
[28] M. Zhou, Y. Zhai, S. Dong, Electrochemical sensing and biosensing platform based on chemically reduced graphene oxide, Anal. Chem. 81 (2009) 5603–5613.
[29] Y. Wang, Y. Shao, D.W. Matson, J. Li, Y. Lin, Nitrogen doped graphene and its application in electrochemical biosensing, ACS Nano 4 (2010) 1790–1798.
[30] D. Cao, P. He, N. Hu, Electrochemical biosensors utilising electron transfer in heme proteins immobilised on Fe_3O_4 nanoparticles, Analyst 128 (2003) 1268–1274.
[31] A.J. Bard, L.R. Faulkner, Electrochemical Methods—Fundamental and Applications, Chapter 6 Potential sweep methods, Wiley, New York, 1980.
[32] S.S. Mandal, K. Karthik Narayan, A.J. Bhattacharyya, Employing denaturation for rapid electrochemical detection of myoglobin using TiO2 nanotubes, J. Mater. Chem. B 1 (2013) 3051–3056.
[33] X. Li, W. Zheng, L. Zhang, P. Yu, Y. Lin, L. Su, L. Mao, Effective electrochemical method for investigation of hemoglobin unfolding based on the redox property of heme groups at glassy carbon electrodes, Anal. Chem. 81 (2009) 8557–8563.
[34] S. Kapoor, S.S. Mandal, A.J. Bhattacharyya, Structure and function of hemoglobin confined inside silica nanotubes, J. Phys. Chem. B 113 (2009) 14189–14195.

[35] S.S. Mandal, S. Bhaduri, H. Amenitsch, A.J. Bhattacharyya, Synchrotron small-angle X-ray scattering studies of hemoglobin non-aggregation confined inside polymer capsules, J. Phys. Chem. B 116 (2012) 9604–9610.
[36] P. Bernabeu, L. Tamisier, A.-D. Cesare, A. Caprani, Study of the adsorption of albumin on a platinum rotating disk electrode using impedance measurements, Electrochim. Acta 33 (1988) 1129–1136.
[37] A. Liu, M. Wei, I. Honma, H. Zhou, Direct electrochemistry of myoglobin in titanate nanotubes film, Anal. Chem. 77 (2005) 8068–8074.
[38] X. Ge, W. Zhang, Y. Lin, D. Du, Magnetic Fe3O4@TiO2 nanoparticles-based test strip immunosensing device for rapid detection of phosphorylated butyrylcholinesterase, Biosens. Bioelectron. 50 (2013) 486–491.
[39] D. Du, Z.X. Zou, Y. Shin, J. Wang, H. Wu, M.H. Engelhard, J. Liu, I.A. Aksay, Y. Lin, Sensitive immunosensor for cancer biomarker based on dual signal amplification strategy of graphene sheets and multienzyme functionalized carbon nanospheres, Anal. Chem. 82 (2010) 2989–2995.
[40] H. Liu, R. Malhotra, M.W. Peczuh, J.F. Rusling, Electrochemical immunosensors for Antibodies to peanut allergen Arah2 using gold nanoparticle–peptide films, Anal. Chem. 82 (2010) 5865–5871.